

Design of ultra-high luminescent polymers for organic photovoltaic cells with low energy loss.

*Jingwen Wang,^{a,b} Lijiao Ma,^{a,b} Young Woong Lee,^c Huifeng Yao,^{*a,d} Ye Xu,^{a,b} Shaoqing Zhang,^d Han Young Woo,^{*c} and Jianhui Hou^{*a,b}*

^a State Key Laboratory of Polymer Physics and Chemistry, Beijing National Laboratory for Molecular Sciences CAS Research/Education Center for Excellence in Molecular Sciences, Institute of Chemistry Chinese Academy of Sciences, Beijing 100190, P. R. China

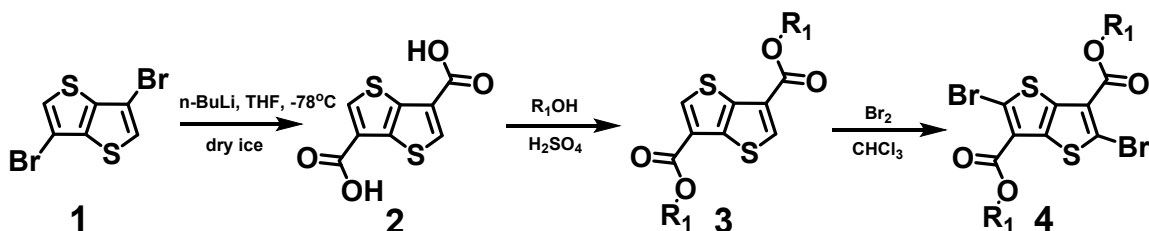
^b University of Chinese Academy of Sciences, Beijing 100049, P. R. China

^c Department of Chemistry, Korea University, Seoul 136-713, Republic of Korea

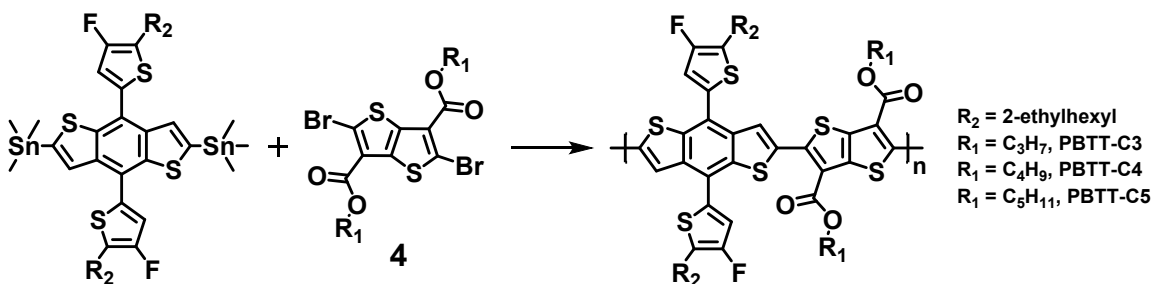
^d School of Chemistry and Biological Engineering, University of Science and Technology Beijing, Beijing 100083, P. R. China

1. Materials and synthesis

All reactions were carried out under argon atmosphere. Monomer BDT-Sn and BTP-eC9 were purchased from Solarmer Materials Inc. Other reagents and solvent were purchased from commercial suppliers and used without further purification. Compounds **1**, **2** and **3** were synthesized according to the literature.²



Synthesis of COTT-2Br (4): To a solution of COTT (**3**) (10 mmol) in 100 ml chloroform, 5 ml Br_2 was slowly added by a syringe. The reaction was stirred at room temperature for 1 hour. Finally, the reaction was quenched using Na_2SO_3 aqueous solution and the crude product was extracted by dichloromethane for three times. After removing the solvent, the residual solid was purified by column chromatography on silica gel with eluent of petroleum ether: chloroform = 1:1 to obtain a white solid with yield of 92%. (COTT-C3-2Br: ^1H NMR (400 MHz, CDCl_3) δ 4.34 (t, $J = 6.5$ Hz, 4H), 1.85 (dt, $J = 14.0, 6.7$ Hz, 4H), 1.09 (t, $J = 7.4$ Hz, 6H); ^{13}C NMR (101 MHz, CDCl_3) δ 160.77, 135.82, 123.60, 76.71, 67.44, 22.01, 10.75. COTT-C4-2Br: ^1H NMR (400 MHz, CDCl_3) δ 4.38 (t, $J = 6.6$ Hz, 4H), 1.86-1.74 (m, 4H), 1.53 (dq, $J = 14.7, 7.4$ Hz, 4H), 1.00 (t, $J = 7.4$ Hz, 6H); ^{13}C NMR (101 MHz, CDCl_3) δ 160.78, 135.82, 123.60, 65.62, 30.62, 19.29, 13.71. COTT-C5-2Br: ^1H NMR (300 MHz, CDCl_3) δ 4.37 (t, $J = 6.6$ Hz, 4H), 1.93-1.70 (m, 4H), 1.59-1.25 (m, 8H), 0.94 (t, $J = 7.0$ Hz, 6H); ^{13}C NMR (75 MHz, CDCl_3) δ 160.77, 135.80, 123.58, 76.61, 65.91, 28.20, 22.28, 13.99.)



Synthesis of PBTT-Cn: BDT-2Sn (0.2 mmol) and COTT-2Br (0.2 mmol) were added into a 25 ml two-necked flask successively. Then 6 ml chlorobenzene was added to dissolve two monomers. After being flushed by a stream of argon for 10 min, Pd(PPh₃)₄ (12 mg, 0.01 mmol) was added. The solution was flushed by argon for another 10 min, and then stirred at 120 °C for 8 hours. After that, the polymer was precipitated in methanol (60 ml). The crude polymer was dried and further purified by Soxhlet extraction with methanol, hexanes, and chloroform. Finally, it was dried in vacuum oven to afford PBTT-Cn (yield: 63%).

2. General methods

The ¹H NMR spectra of PBTT-C3 and C4 were obtained from a BRUKER AVANCE III 400 MHz spectrometer in CDCl₃ at 298 K. The ¹³C NMR spectra of them were obtained from the same instrument with a frequency of 101 MHz in CDCl₃ at 298 K. While for PBTT-C5, a BRUKER Fourier 300 spectrometer was used to obtain ¹H NMR spectrum. The ¹³C NMR spectra of it were obtained from the same instrument with a frequency of 75 MHz in CDCl₃ at 298 K. UV-Vis absorption spectra of films (spin-coated on quartz substrates) were taken on a Hitachi UH5300 UV-Vis spectrophotometer, and temperature-dependent UV-Vis absorption spectra of polymer solutions were recorded on a Hitachi UH4150 spectrophotometer. The electrochemical cyclic voltammetry was conducted using a CHI650D electrochemical workstation, and glassy-carbon, platinum-wire and Ag/Ag⁺ electrode were acted as working electrode, counter electrode, and reference electrode, respectively. 0.1 M tetrabutylammonium hexafluorophosphate (Bu₄NPF₆) acetonitrile solution was utilized as the electrolyte. After completing the measurement, ferrocene was measured as an internal standard (absolute energy level of 4.8 eV below vacuum). ($HOMO = -(4.8 + E_{ox} - E(Fc/Fc^+))$ eV, $LUMO = -(4.8 + E_{red} - E(Fc/Fc^+))$ eV).

3. Devices fabrication and characterization

Conventional device structure (glass/ITO/PEDOT:PSS/PBTT-Cn:BTP-eC9/PFN-Br/Al) was used to fabricate OPV cells. ITO-coated glass was purchased from South China Xiang's Science & Technical Company Limited. PEDOT:PSS (4083) was purchased from the Clevios™. BTP-eC9 and PFN-Br were purchased from Solarmer Material Inc. PEDOT:PSS was diluted with the same volume of water. PFN-Br was dissolved in methanol with a concentration of 0.5 mg/ml. PBTT-C4:BTP-eC9 (D/A 1:1.2) were dissolved in *o*-xylene at the polymer concentration of 6 mg/ml. PBTT-C3:BTP-eC9 (D/A 1:1.2) were dissolved in *o*-xylene at the polymer concentration of 4 mg/ml and PBTT-C5:BTP-eC9 (D/A 1:1.2) were dissolved in *o*-xylene at the polymer concentration of 10 mg/ml. All the solutions should be stirred at 80 °C for at least 2 h. Before spin-coating the active layer, 0.5% 1-chloronaphthalene (v/v) was added to mixed solutions. After stirring for another 30 mins, solar cells were fabricated by the following conditions: Firstly, about 10 nm PEDOT:PSS layers were spin-coated on the pre-cleaned ITO substrates and annealed at 150 °C for 15 min. Subsequently, the substrates were transferred to the glove box. The substrates were placed on a hotplate at 80 °C. The mixed solutions were spin-coated onto the PEDOT:PSS layers, and then the films were treated with the thermal annealing at 100 °C for 10 min. The best active layer thickness is about 120 nm. PFN-

Br was spin-coated onto active layers at 3000 rpm for 30 s. Finally, 100 nm Al was deposited under a high vacuum. The areas of the masks are about 0.037 cm² in our laboratory.

Space charge limited current (SCLC) measurements were conducted on single-carrier devices. The structure of hole-only and electron-only devices is ITO/PEDOT:PSS/active layer/Au/Al and electron-only, ITO/ZnO/active layer/PFN-Br/Al, respectively. The mobilities was calculated by the Mott-Gurney

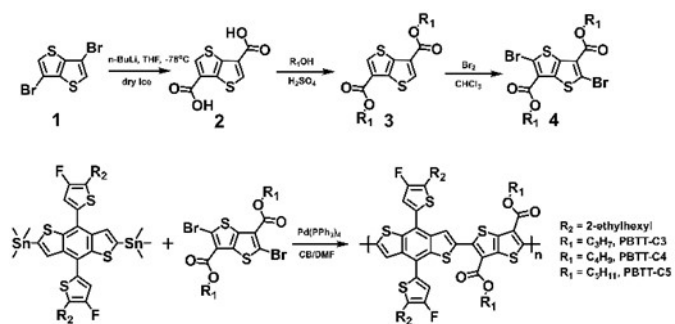
equation: $J = \frac{9}{8} \epsilon_0 \epsilon_r \mu \frac{V^2}{d^3}$. The J - V measurements were performed by using the solar simulator (SS-F5-3A, Enlitech) along with AM 1.5G spectra (100 mW/cm²). The EQE spectra were measured through the Solar Cell Spectral Response Measurement System QE-R3011 (Enli Technology Co., Ltd., Taiwan). Absorption spectra of the materials were measured on a Hitachi UH5300 spectrophotometer. All absorbent samples (solutions and films) of NFAs were prepared using *o*-xylene as a solvent. The photo-CELIV measurements were performed by the all-in-one characterization platform Paios developed and commercialized by Fluxim AG, Switzerland. Highly Sensitive EQE was measured by using an integrated system (PECT-600, Enlitech), where the photocurrent was amplified and modulated by a lock-in instrument. Electroluminescence (EL) quantum efficiency (EQE_{EL}) measurements were performed by applying external voltage/current sources through the devices (ELCT-3010, Enlitech). AFM height and phase images were recorded on a Nanoscope AFM microscope (Bruker), where the tapping mode was used. The samples were fabricated in accordance with the conditions of the best devices. Grazing incident wide-angle x-ray scattering (GIWAXS) measurements were performed at the 9A beamline in the Pohang Accelerator Laboratory (PAL)); the energy, pixel size, wavelength, and scanning interval at the 9A beamline were 11.075 keV, 79.59 μm, 1.11946 Å, and 2θ = 0°–20°, respectively. The scattering vectors, q_{xy} and q_z were respectively parallel and perpendicular to the substrate. Polymer samples were prepared on Si substrates using identical spin speeds, solvents, concentrations, and annealing temperatures and times as for the relevant OPV devices.

4. Calculation

The molecular geometries were optimized by Gaussian 09 with a functional of B3LYP and a basis set of 6-31G(d,p).² The long alkyl chains were replaced by methyl for saving computation time. Then the methyl was replaced with the real alkyl chain, a polymer chain was constructed with 8 repeating units. A 30 nm × 30 nm × 30 nm box with periodic boundary conditions (PBC) was built to simulate the solution state using Packmol software.³ The box consisted of two polymer chains and 12000 *o*-xylene molecules. All-atom molecular dynamics (MD) simulations were performed using Gromacs-2019.4.⁴ The Optimized Potentials for Liquid Simulations – All Atom (OPLS-AA) was adopted to describe the interactions between atoms.^{5,6,7} Atomic charges were calculated from the restrained electrostatic potentials (RESP) at the B3LYP/6-311G(d,p) level of theory using Multiwfn program.^{8,9} During the simulations, Berendsen pressure coupling, velocity rescaling thermostat, and timestep of 2 fs were used. The short-range electrostatics and van der Waals interactions were truncated at 1.0 nm. The long-range electrostatics interactions were summed using particle mesh Ewald

(PME) method. The simulated system was firstly energy-minimized and equilibrated for 6 ns under the NPT ensemble at 303K with atmospheric pressure. The box size changed slightly to reach a stable density. Then, 4-ns production simulations were performed under the NPT ensemble at 303K with a sampling interval of 2 ps.

Results and Discussion



Scheme S1. Synthesis route of PBTT-C_n polymers.

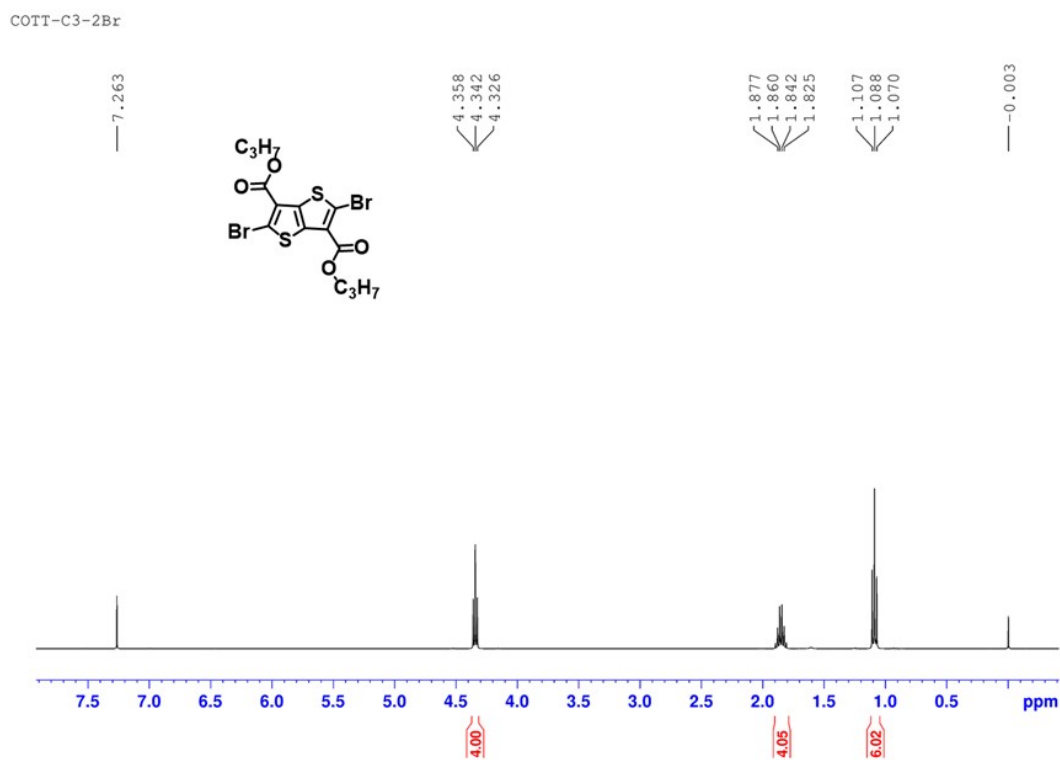


Fig S1. ¹H NMR of COTT-C3-2Br

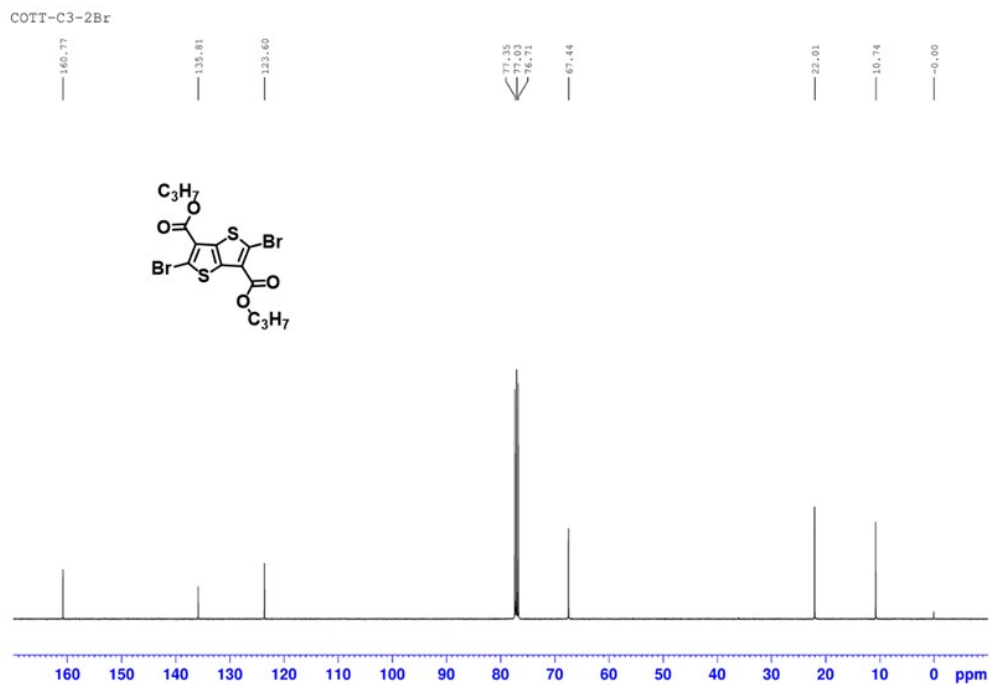


Fig S2. ^{13}C NMR of COTT-C3-2Br

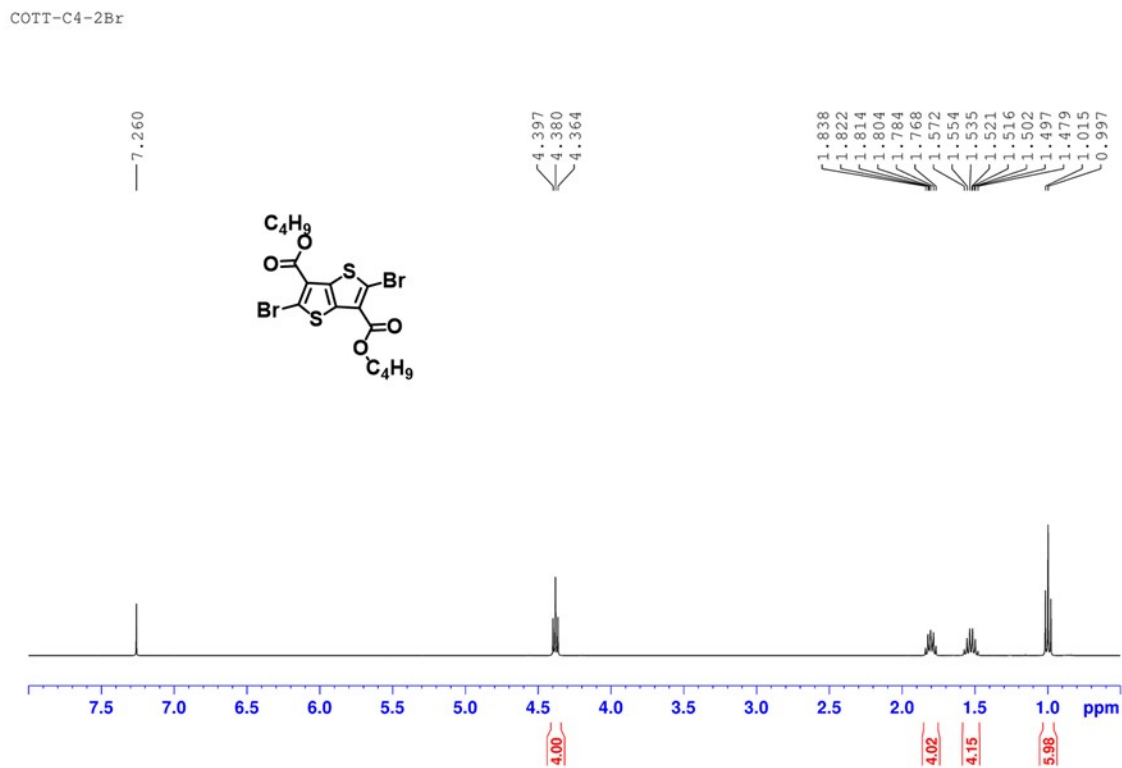


Fig S3. ^1H NMR of COTT-C4-2Br

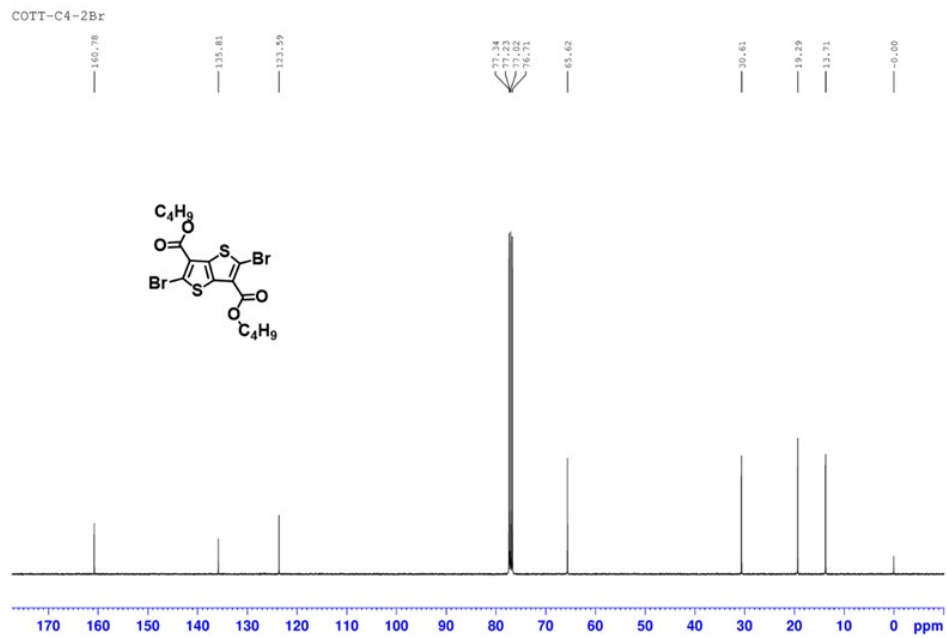


Fig S4. ^{13}C NMR of COTT-C4-2Br

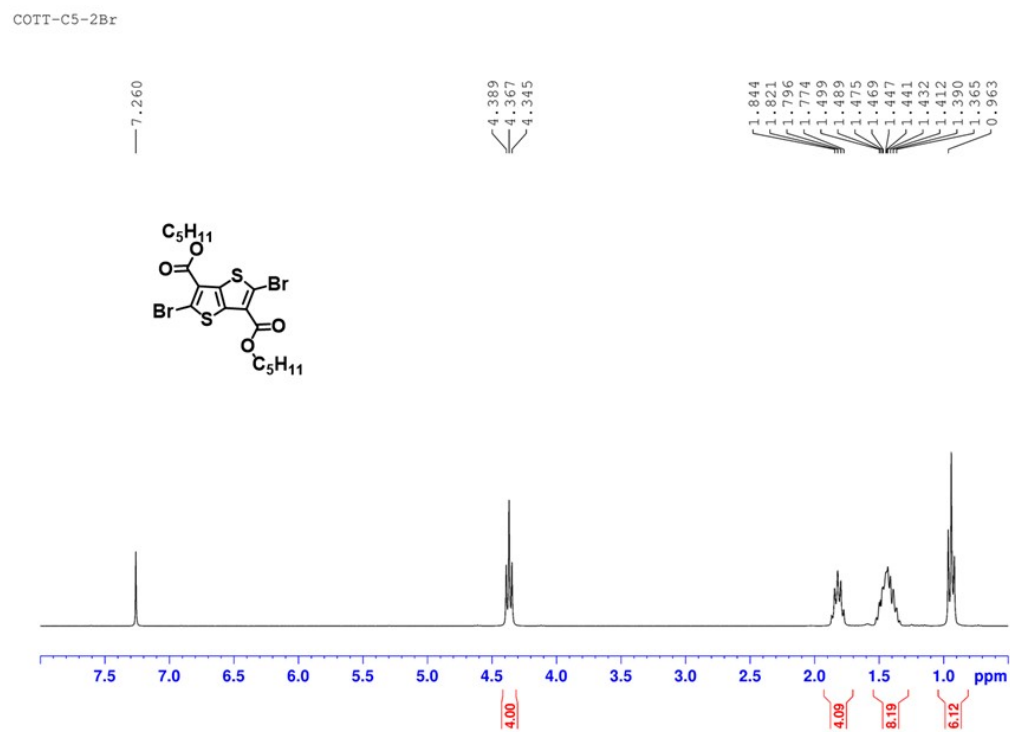


Fig S5. ^1H NMR of COTT-C5-2Br

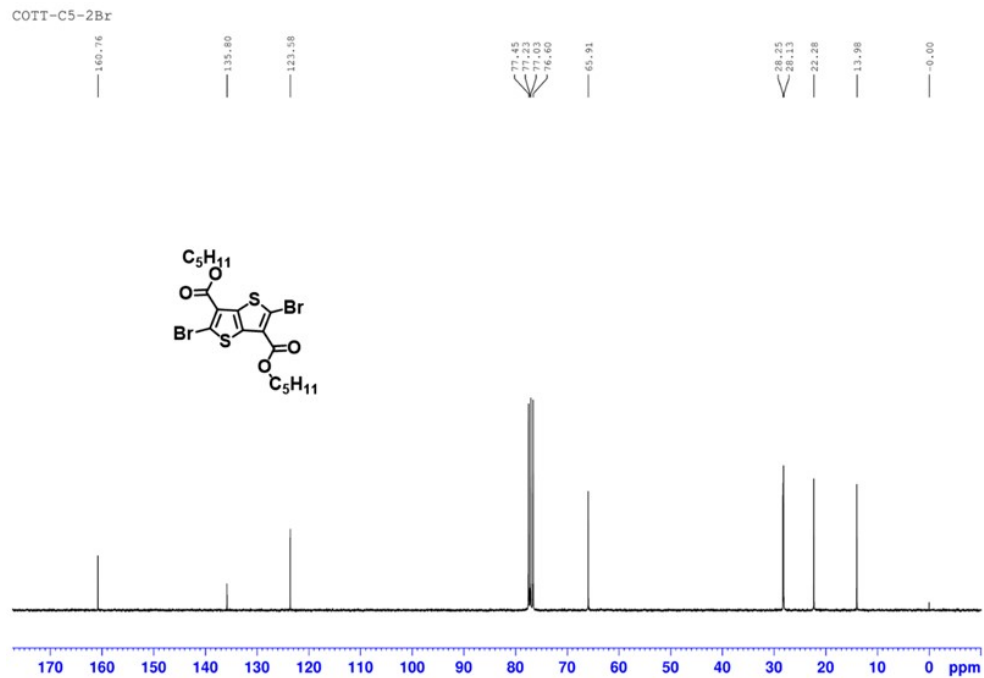


Fig S6. ^{13}C NMR of COTT-C5-2Br

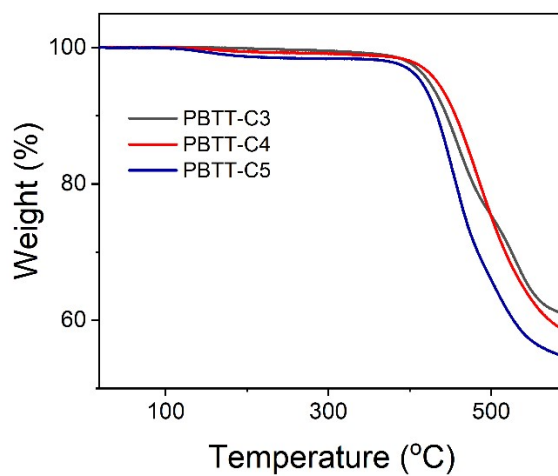


Fig S7. The thermal gravimetric analysis (TGA) curves under the N_2 atmosphere.

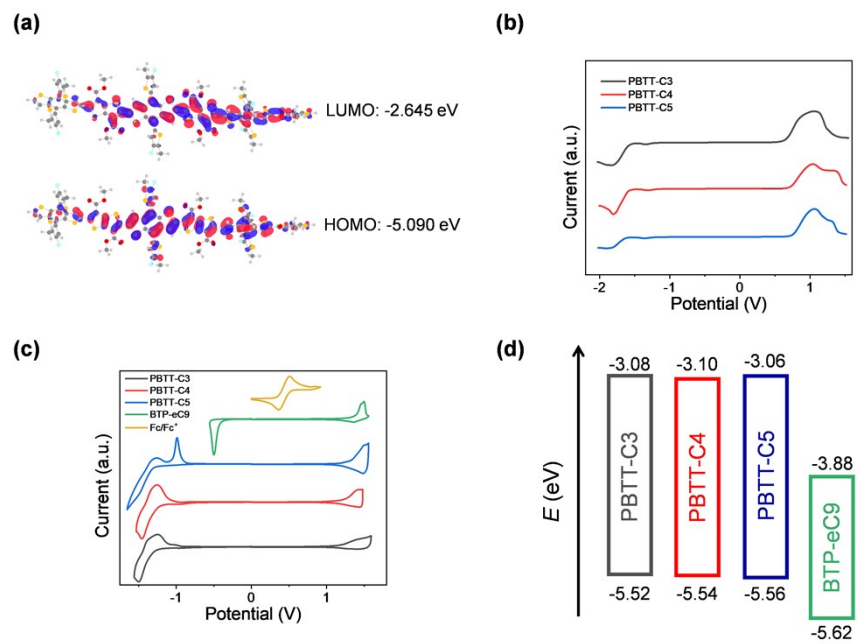


Fig S8. The calculated LUMO and HOMO (a) distributions of PBTT-Cn trimer. (b) SWV curves of three polymers. (c) Cyclic voltammograms curves of three PBTT-Cn polymers and BTP-eC9. (Fc/Fc⁺ as the Internal standard) (d) Energy level diagrams of three polymers and BTP-eC9.

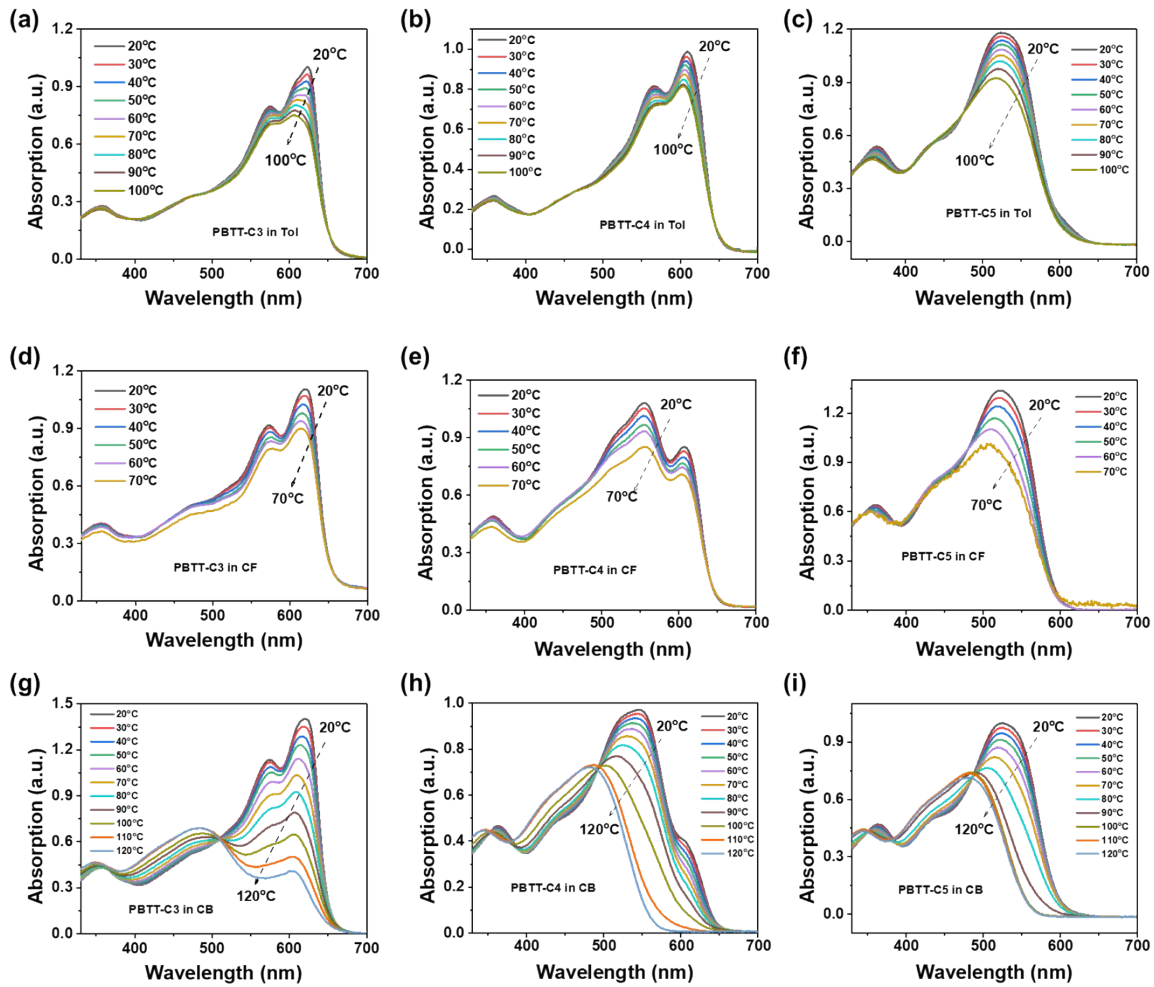


Fig S9. TD UV-vis absorption of PBTT-C3 (a, d, g), PBTT-C4 (b, e, h), PBTT-C5 (c, f, i) in Tol, CF and CB solution, respectively.

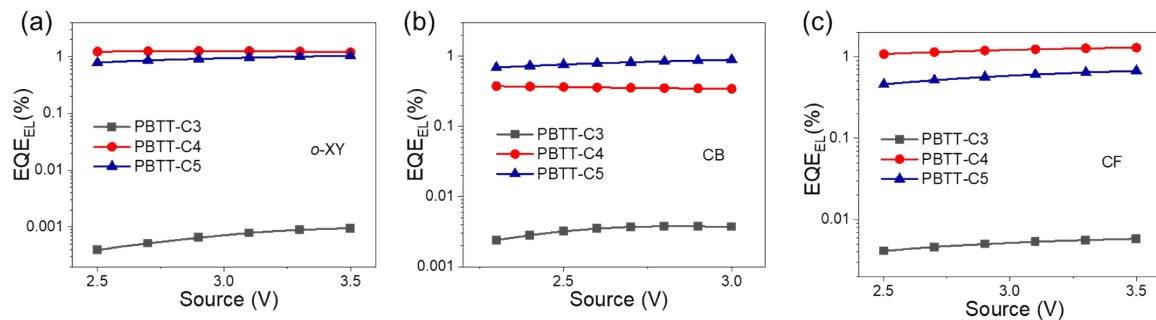


Fig S10. EQE_{EL} spectra of pristine PBTT-C_n-based film by using *o*-XY (a), CB (b) and CF (c) as processing solvent.

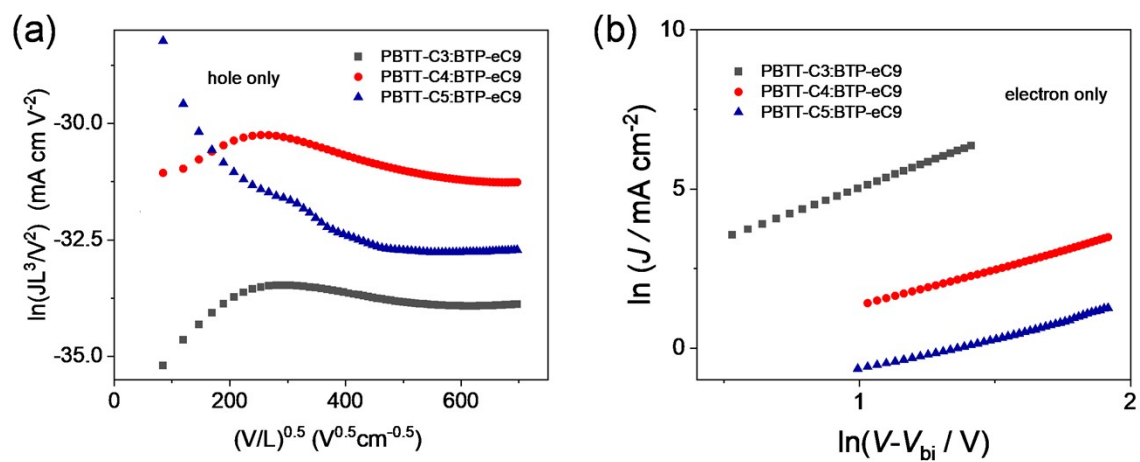


Fig S11. (a) Hole mobilities of three PBTT-C_n-based blend films. (b) Electron mobilities of polymer blend films.

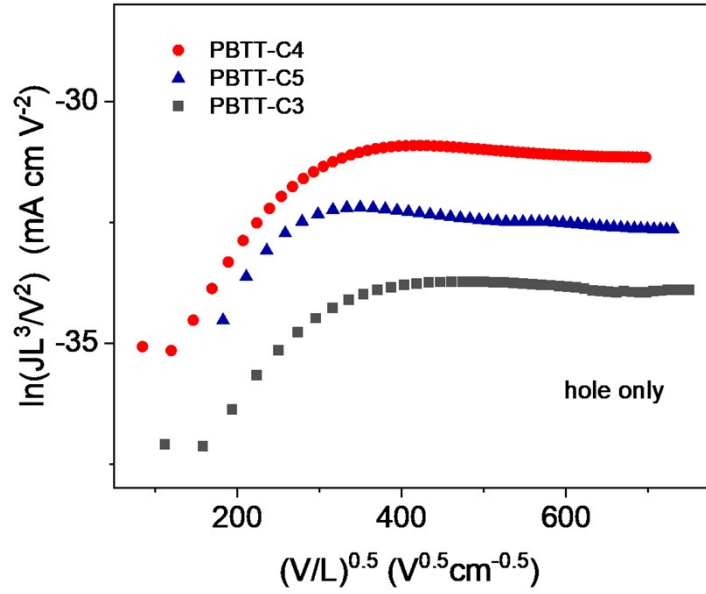


Fig S12. Hole mobilities of three pure polymer-based films.

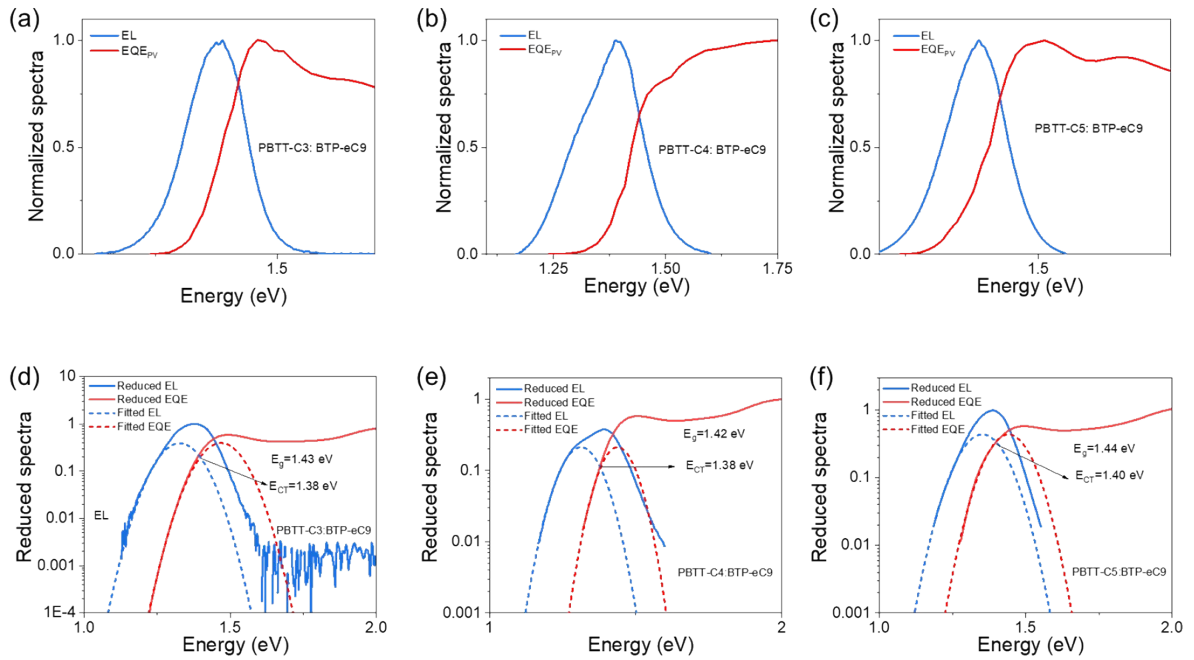


Fig S13. E_g determination of PBTT-C3:BTP-eC9 (a), PBTT-C4:BTP-eC9 (b) and PBTT-C5:BTP-eC9 (c) using the crossing point of normalized EL and EQE spectra. The determination of E_{CT} s of PBTT-C3:BTP-eC9 (d), PBTT-C4:BTP-eC9 (e), PBTT-C5:BTP-eC9 (f) of Reduced EL and EQE.

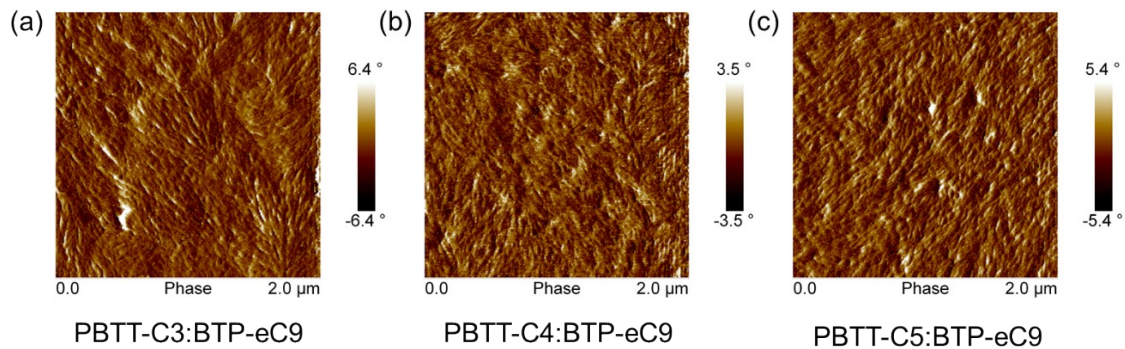


Fig S14. AFM phase images of PBTT-C3:BTP-eC9 (a), PBTT-C4:BTP-eC9 (b) and PBTT-C5:BTP-eC9 (c) films.

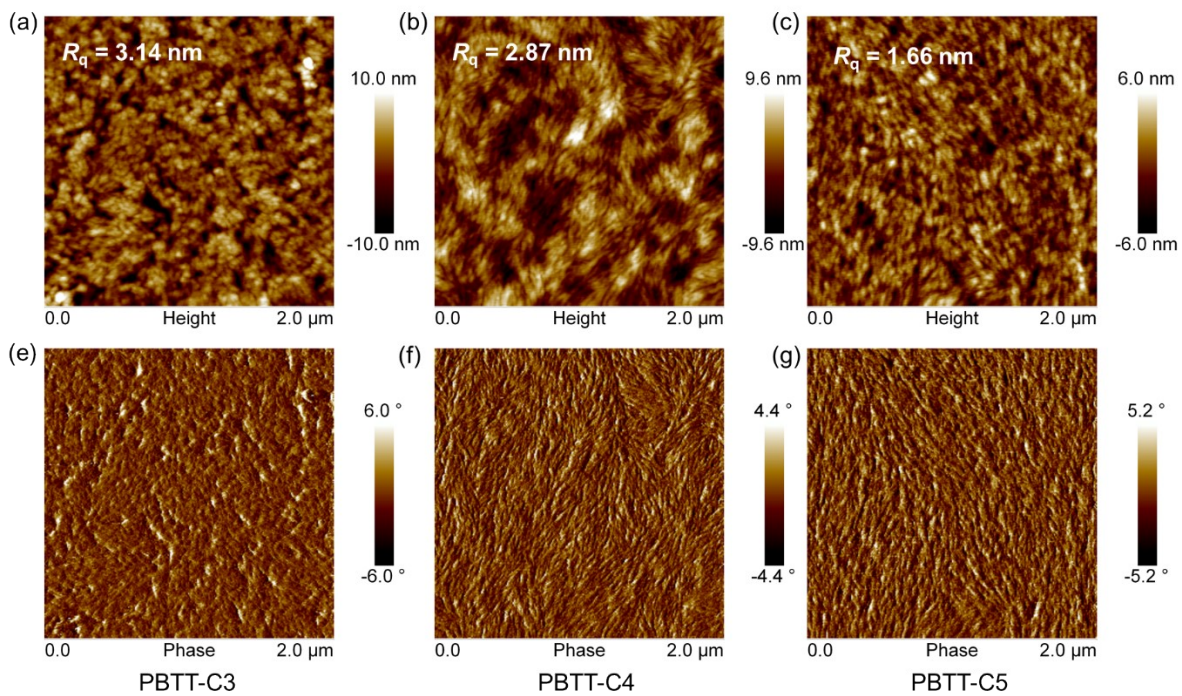


Fig S15. AFM height images of pristine PBTT-C3 (a), PBTT-C4 (b), PBTT-C5 (c) films. AFM phase images of pristine PBTT-C3 (d), PBTT-C4 (e), PBTT-C5 (f) films.

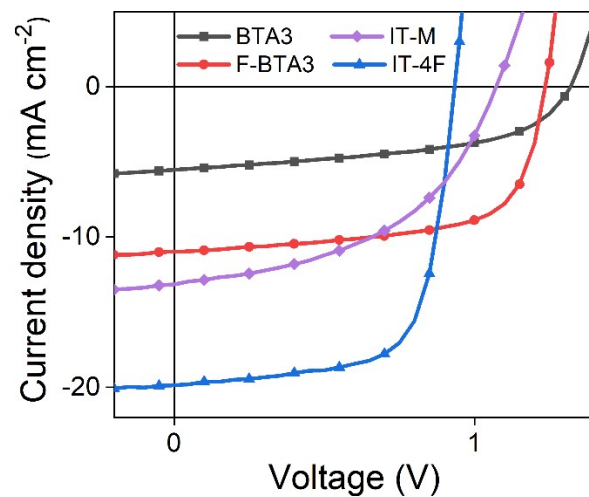


Fig S16. J - V curves of devices based on PBTT-C4 and other NFAs.

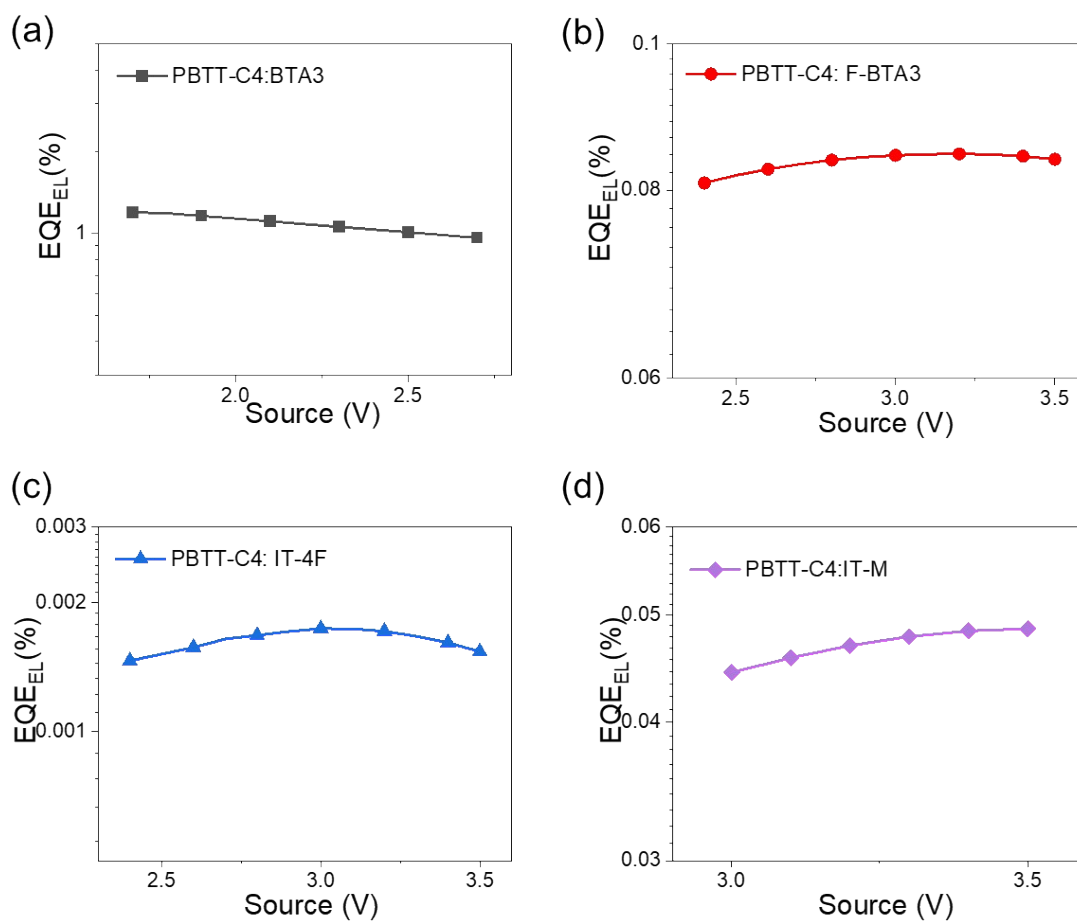


Fig S17. EQE_{EL} of devices based on PBTT-C4 and other NFAs.

Table S1. Mobilities of PBTT-Cn:BTP-eC9-based and pure polymers-based devices based on methods of SCLC.

Combination	$\mu_h(\text{cm}^2\text{V}^{-1}\text{s}^{-1})$	$\mu_e(\text{cm}^2\text{V}^{-1}\text{s}^{-1})$	μ_h/μ_e
PBTT-C3:BTP-eC9	1.03×10^{-5}	4.27×10^{-5}	0.24
PBTT-C4:BTP-eC9	3.13×10^{-4}	1.58×10^{-4}	1.98
PBTT-C5:BTP-eC9	5.33×10^{-5}	1.14×10^{-5}	4.68
PBTT-C3	1.32×10^{-5}		
PBTT-C4	2.18×10^{-4}		
PBTT-C5	6.65×10^{-5}		

Table S2. Voltage loss profiles of the PBTT-Cn-based devices.

Active Layer	E_g (eV)	V_{oc} (V)	E_{loss} (eV)	E_{CT} (eV)	ΔE_{CT} (eV)	$\Delta V_{non-rad}$ (V)	ΔV_{rad} (V)
PBTT-C3: BTP-eC9	1.43	0.657	0.773	1.38	0.05	0.289	0.434
PBTT-C4: BTP-eC9	1.42	0.892	0.528	1.38	0.04	0.190	0.298
PBTT-C5: BTP-eC9	1.44	0.887	0.553	1.40	0.04	0.212	0.301

Table S3. Photovoltaic parameters of devices based on PBTT-C4 and other NFAs.

Acceptor	V_{oc} (V)	J_{sc} (mA/cm ²)	FF (%)	PCE (%)	EQE _{EL} (%)	$V_{loss}^{non-rad}$
BTA3	1.32	5.83	51.4	3.96	1.20	0.11
F-BTA3	1.23	11.0	65.6	8.88	0.0846	0.18
IT-4F	0.934	19.9	69.0	12.8	0.00174	0.28
IT-M	1.07	12.3	52.4	6.90	0.0486	0.20

Reference

1. Y. Wang, H. Guo, S. Ling, I. Arrechea-Marcos, Y. Wang, J. T. López Navarrete, R. P. Ortiz and X. Guo, Ladder-type Heteroarenes: Up to 15 Rings with Five Imide Groups, *Angewandte Chemie International Edition*, 2017, **56**, 9924-9929.
2. M. J. Frisch, G. W. Trucks, H. B. Schlegel, G. E. Scuseria, M. A. Robb, J. R. Cheeseman, G. Scalmani, V. Barone, B. Mennucci, G. A. Petersson, H. Nakatsuji, M. Caricato, X. Li, H. P. Hratchian, A. F. Izmaylov, J. Bloino, G. Zheng, J. L. Sonnenberg, M. Hada, M. Ehara, K. Toyota, R. Fukuda, J. Hasegawa, M. Ishida, T. Nakajima, Y. Honda, O. Kitao, H. Nakai, T. Vreven, J. A. Montgomery Jr., J. E. Peralta, F. Ogliaro, M. J. Bearpark, J. Heyd, E. N. Brothers, K. N. Kudin, V. N. Staroverov, R. Kobayashi, J. Normand, K. Raghavachari, A. P. Rendell, J. C. Burant, S. S. Iyengar, J. Tomasi, M. Cossi, N. Rega, N. J. Millam, M. Klene, J. E. Knox, J. B. Cross, V. Bakken, C. Adamo, J. Jaramillo, R. Gomperts, R. E. Stratmann, O. Yazyev, A. J. Austin, R. Cammi, C. Pomelli, J. W. Ochterski, R. L. Martin, K. Morokuma, V. G. Zakrzewski, G. A. Voth, P. Salvador, J. J. Dannenberg, S. Dapprich, A. D. Daniels, Ö. Farkas, J. B. Foresman, J. V. Ortiz, J. Cioslowski, D. J. Fox, *Gaussian 09*; Gaussian, Inc.: Wallingford, CT, 2009.
3. L. Martínez, R. Andrade, E. G. Birgin, J. M. Martínez, *J. Comput. Chem.* 2009, **30**, 2157
4. M. J. Abraham, T. Murtola, R. Schulz, S. Páll, J. C. Smith, B. Hess, E. Lindahl, *SoftwareX* 2015, **1–2**, 19.
5. Jorgensen, W.L., and Tirado-Rives, J. The OPLS [optimized potentials for liquid simulations] potential functions for proteins, energy minimizations for crystals of cyclic peptides and crambin. *J. Am. Chem. Soc.* 1988 **110**, 1657-1666.
6. Dahlgren, M.K., Schyman, P., Tirado-Rives, J., and Jorgensen, W.L Characterization of biaryl torsional energetics and its treatment in OPLS all-atom force fields. *J. Chem. Inf. Model.* 2013 **53**, 1191-1199.
7. Jackson, N.E., Kohlstedt, K.L., Savoie, B.M., de la Cruz, M.O., Schatz, G.C., Chen, L.X., and Ratner, M.A. Conformational order in aggregates of conjugated polymers. *J. Am. Chem. Soc.* 2015 **137**, 6254-6262.
8. C. I. Bayly, P. Cieplak, W. D. Cornell, P. A. Kollman, *J. Phys. Chem.* 1993, **97**, 10269.
9. T. Lu, F. Chen, *J Comput Chem* 2012, **33**, 580-592.